Swiss J Palaeontol (2015) 134:207–216
DOI 10.1007/s13358-015-0083-0

Non-invasive imaging techniques combined with morphometry: a case study from *Spirula*

René Hoffmann[1] · Daniel Reinhoff[1] · Robert Lemanis[1]

Received: 10 March 2015 / Accepted: 19 May 2015 / Published online: 10 June 2015

Abstract *Spirula spirula* is a unique deep-sea squid with unknown taxonomic status. Precise description of shell morphology may help to decide whether the genus contains one or more species. Here, a straight forward description of ontogenetic changes of shell parameters is presented for a single shell of *Spirula spirula*. Using micro-computed tomography, surface and volumetric data, e.g., chamber volumes and surface areas, as well as siphuncle volumes and surface areas were collected and used for the description. Advantage of the method, combining non-invasive imaging techniques with classical morphometry, is discussed.

Keywords Computed tomography · Species description · Cephalopod shells · 2D and 3D Conch features

Introduction

Cephalopods are, due to their accretionary shell growth, ideal candidates to study ontogenetic changes, intraspecific variability, and macro-evolutionary patterns. However, most of the recent cephalopods, namely the coleoids, have reduced shells with two exceptions: *Sepia* and *Spirula*. For the *Sepia*, many different species have been described, while for *Spirula*, the taxonomic status is still under debate. Earlier workers have described several species for *Spirula* from different localities based on only a few and mostly incomplete specimens. Subsequently, all species have been synonymized under *Spirula spirula* (Linnaeus, 1758), i.e., *Spirula* today is recognized as a monospecific genus (see Warnke 2007; Lukeneder et al. 2008; Haring et al. 2012). Repository of the type species remains unclear, and Linné did not designate a holotype for his "*Nautilus spirula*". Some syntypes of *Spirula spirula* are deposited in the Linnean Society in London (http://linnean-online.org/17140/), but some are probably in Rome, Pisa, Florence, and Gdańsk (pers. comm. Svetlana Nikolaeva). Cephalopod species, including *Spirula*, were traditionally differentiated from each other utilizing a static ("Linnean") rather than a dynamic ("Darwinian") approach. This static method does not account for intraspecific variation, covariation, or ontogenetic changes. Many species were thus erected on the basis of subtle morphological differences of the adult stage, which is in contrast to the known high degree of intraspecific variability in shape and ornamentation of many molluscs especially the sister taxon of the Cephalopoda: the Gastropoda (Samadi et al. 2000; Scholz and Glaubrecht 2010; Teso et al. 2011). During the last two decades, the description of cephalopod shells, mainly promoted by ammonite workers, has changed significantly. The description of ontogenetic trajectories as well as the use of intraspecific variability analyses of a "population" (=a number of specimens from a single bed) has become common (Hohenegger and Tatzreiter 1992; Dagys and Weitschat 1993; Tanabe 1993; Hammer and Bucher 2005; Korn and Klug 2007; Landman et al. 2010; Monnet et al. 2010; De Baets et al. 2012). Most of the shell-bearing cephalopod species (extinct and recent) are not characterized by apomorphic characters but by a combination of quantitative characters. Therefore, species diagnosis is often composed of a set of characters that allow the

✉ René Hoffmann
rene.hoffmann@rub.de

[1] Department of Earth Sciences, Institute of Geology, Mineralogy, and Geophysics, Branch Paleontology, Ruhr-Universität Bochum, Universitätsstrasse 150, 44801 Bochum, Germany

comparison between species usually containing characters of conch morphology and ontogeny, and suture line (Ruzhencev 1960; Kutygin 1998; Korn 2010). Recently, two attempts were made to clarify the taxonomic status of *Spirula*, the first focused on molecular data (Warnke 2007; Haring et al. 2012) and the second applied the morphometric approach (Neige and Warnke 2010; Lukeneder, this volume). Both approaches challenged the monospecific status of *Spirula* but could not demonstrate the existence of two or more species.

Herein, a standardized method of character description and conch form analysis is applied to a single *Spirula* shell. The extraordinary conch shape, deviating from a planispiral morphology, requires the consideration of additional conch parameters (see "Materials and methods"). For the first time, the morphometric approach is combined with non-invasive imaging techniques, namely micro-computed tomography. It is demonstrated here that volume data of a distinct geometry can significantly improve morphological descriptions. The aims of this study are the following: (a) to show that CT data can provide more information about the shell geometry compared to traditional approaches, which are limited to 180° or 90° plane cuts, while CTdata can be virtually cut every 10°, (b) besides traditional 2D-measurements of the external shell geometry, 2D-measurements of internal structures and 3D-measurements like chamber or siphuncle volumes and surface areas become available and can be compared (in case more specimens become available) for ontogenetic trends or intra- and interspecific variability without destroying the examined specimen, and (c) high-resolution scans provide data with sufficient precision to recognize minute changes in 2D- and 3D-measurements (Fig. 1a–c).

Materials and methods

We analyzed a single shell of the deep-sea squid *Spirula spirula* (Decabrachia, Coleoidea) that washed ashore at Fuerteventura (Canary Islands) off Northwest Africa (leg. Kerstin Warnke). The shell has a maximum diameter of 17.6 mm, and the initial chamber (=protoconch) is preserved. The shell contains 30 chambers in total. The shell was scanned at the GeoForschungsZentrum Potsdam with a GE Phoenix|x-ray nanotom-s®, a micro-computed tomograph device equipped with a 180 kV nanofocus tube, with a resolution of 8.7 µm. Amira® was used for the analysis of the tomographic data. Since the *Spirula* shell resembles that of Devonian and Cretaceous heteromorph ammonoids, the description of conch geometry largely follows Korn and Klug (2007), De Baets et al. (2009, 2013), Korn (2010), and Naglik et al. (2015). Data for conch characteristics were obtained from longitudinal and cross sections for every 10° (Fig. 2). Following Neige and Warnke (2010), we used the same anatomical landmark (dorsal attachment of the first septum) as the shell center (Fig. 1c). Besides morphometry, CT data are used for volumetric analyses, e.g., chamber volumes, as well (Fig. 1b).

For a consistent data description, the largest parameter, e.g., the diameter, is abbreviated with dm_1, while the parameter exactly 180° (or half a whorl) earlier is abbreviated with dm_2.

Basic conch parameters are the conch diameter (dm; dm_1, dm_2), whorl width (ww; ww_1, ww_2), whorl height (wh; wh_1, wh_2), and whorl interspace (wi; wi_1, wi_2). All values of basic conch parameters are given in mm.

Finally, the following conch proportions and expansion rates (growth rates) can be computed:

$$\text{Umbilical width (uw)} = dm_1 - wh_1 - wh_2$$

$$\text{Whorl expansion rate (WER)} = [dm_1/(dm_1 - wh_1 - wi_1)]^2$$

$$\text{Whorl width expansion rate (WWER)} = (ww_1/ww_2)^2$$

$$\text{Whorl height expansion rate (WHER)} = (wh_1/wh_2)^2$$

$$\text{Umbilical width index (UWI)} = uw_1/dm_1$$

$$\text{Conch width index (CWI)} = ww_1/\ dm_1$$

$$\text{Conch height index (CHI)} = wh_1/dm_1$$

(=WHI of De Baets et al. 2013)

$$\text{Whorl width index (WWI)} = ww_1/wh_1$$

$$\text{Whorl interspace index (WII)} = wi_1/wh_1$$

Septal spacing, presented in angles, was quantified by using two different methods:

SDW = number of septa per 180 degrees or half a whorl

ASI_{20} = absolute septal index

The ASI refers to the number of septa counted along the ventral shell margin within a circle of 20 mm in diameter, which is perfectly aligned to the point where the whorl height is measured (Fig. 2). Similar to the quantifiers for rib spacing introduced by De Baets et al. (2013), the ASI is less influenced by coiling variability than SDW, and the SDW averages out possible short-term variation in septal spacing.

Chamber and siphuncle volumes are presented for each chamber as linear plots. Chambers were segmented as individual volumes, while the continuous siphuncle was artificially divided into segments corresponding with the respective chamber length measured as the linear distance between septa (Fig. 1b). Segmentations were performed using Amira®. See Hoffmann et al. (2014) and Lemanis

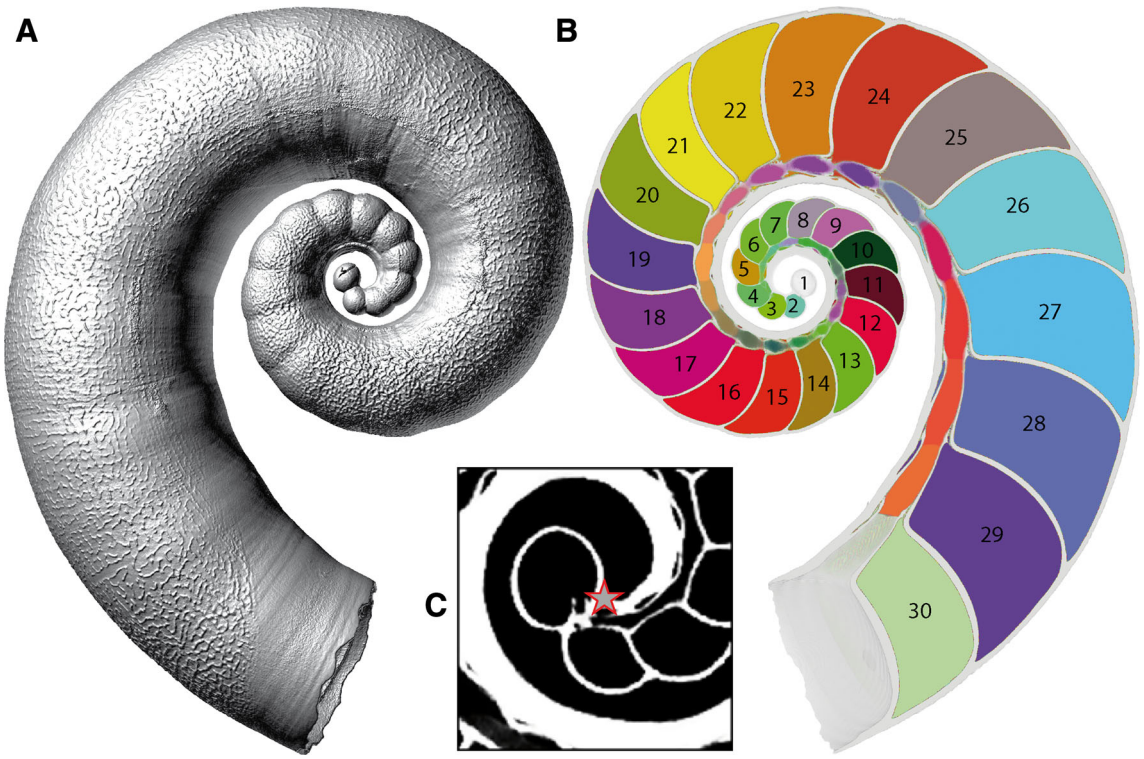

Fig. 1 *Spirula spirula* images based on micro-CT data. **a** Surface rendering showing every minute detail of the shell surface. **b** Median section of the shell with different colors for every single chamber volume and siphuncle volume. **c** Close up of *B* to show the position of the anatomical landmark used to define the center of the shell (*star* at the dorsal attachment of the first septum to the shell, Neige and Warnke 2010)

et al. (2015) for the calculation of volumes based on CT data. Finally, the Chamber-Siphuncle index (CSI) is introduced and is defined as the ratio between the chamber volume and the siphuncle surface area. The CSI is a measure of the relative time necessary to empty a chamber. The index depends on the previous chamber being emptied of some liquid before the next chamber formation can begin and the rate of emptying, which largely depends on the siphuncular surface area.

Besides the ultrastructure of the siphuncle, the osmotic pump mechanism additionally depends on the hydrostatic pressure and the diameter of the siphuncle which is limited by strength requirements (see Hoffmann et al. 2015 for review).

External 2D-measurements are presented as logarithmic plots, while most internal 2D-measurements are presented as linear plots except for ASI20 and SDW (Fig. 4e). Volumes are plotted against chamber number and not against diameter in a linear bivariate plot except for chamber volumes plotted against septal angle.

Results

2D External morphology

Bivariate plots of the whorl height and whorl width show similar trends during ontogeny (Fig. 3a–b). However, the whorl width index (WWI) reveals that the shell is higher than wide at a diameter of 3 mm, wide as high at a diameter of 5 mm, wider than high at a diameter of 15 mm with the highest ww/wh ratio at 10 mm and ends with a nearly circular cross section at the largest shell diameter (Fig. 3c). In this context, the WHER and WWER show similar trends (Fig. 3d–e). The conch width index (CWI) shows at first a decreasing followed by an increasing trend (at 3-mm diameter). From 3- to 9-mm diameter, the CWI remains unchanged followed by a constant decrease till the end of the shell. A similar trend was obtained for the conch height index (CHI) of this specimen (Fig. 3f–g). The WWI, WHER, WWER, and CWI show a larger scatter during the early ontogeny (Fig. 3c–f).

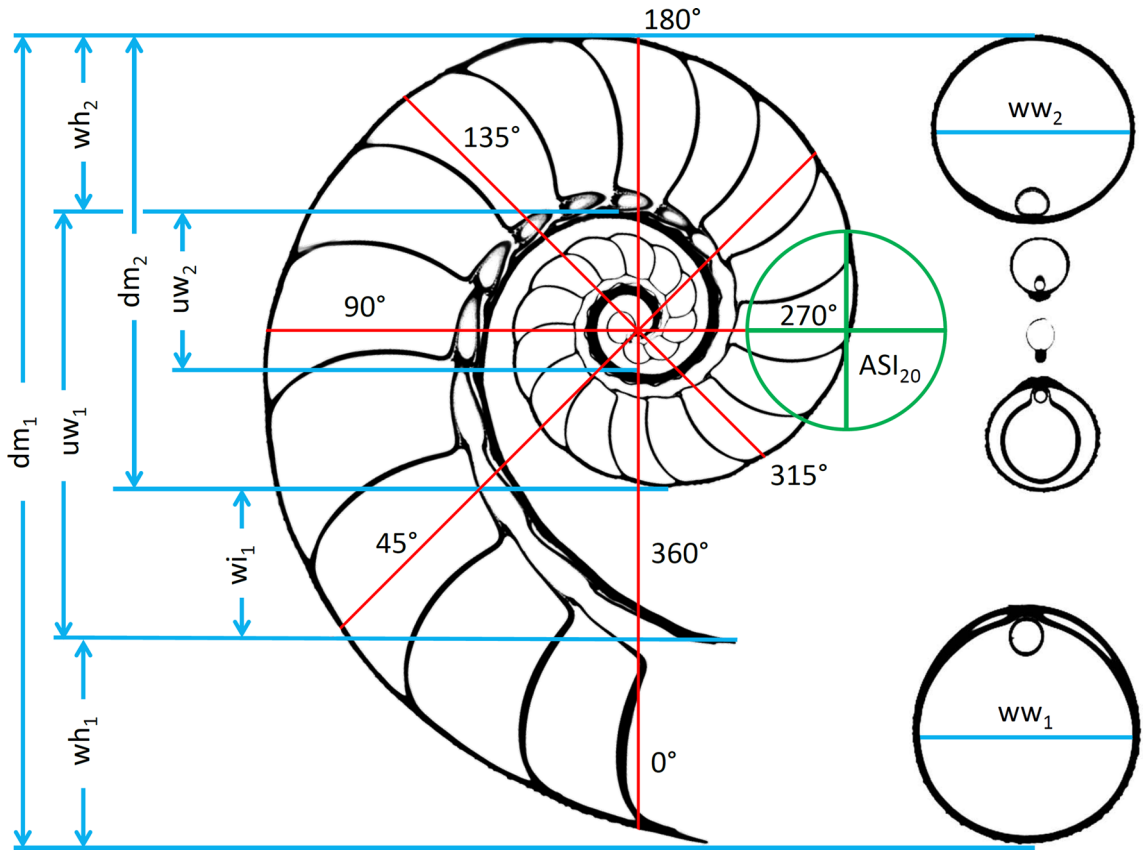

Fig. 2 Median and cross section of the *Spirula spirula* shell with conch dimensions used to calculate conch proportions and expansion rates (ASI_{20} circle not to scale)

The whorls of the *Spirula* shell are not in contact leaving a whorl interspace (wi) of variable dimension between the whorls. The wi shows a repeatedly increasing and decreasing trend for the first 10 mm. At a diameter of 10 mm, this trend becomes less pronounced and finally disappears during the final phase of shell secretion due to the opening of the shell, which leads to the constantly increasing wi (Fig. 3h). This trend is much more pronounced in the whorl interspace index (WII). However, the WII shows a decreasing trend (5–10-mm diameter), which describes the stage when the increase of the wi exceeds the increase in diameter (Fig. 4a). The umbilical width shows a nearly linear increasing trend with a slightly steeper slope during the end of ontogeny (Fig. 4b). That change is clearly related with the increased wi. The umbilical width index (UWI) shows a steep increase between 3- and 5-mm diameter, a plateau phase between 5- and 6-mm diameter, and then again an increase from seven to 15-mm diameter. The curve becomes slightly steeper over the remaining part of the shell (Fig. 4c). The last shell character derived from external shell features is the WER, which shows a large scatter for the earliest juvenile phase. At a diameter of about 5 mm, the WER is constantly decreasing with a slight increase during the final stage (Fig. 4d).

2D Internal morphology

ASI_{20} values were calculated for a shell diameter larger than 10 mm because early shell parts were completely included within a circle of 20 mm and therefore do not represent comparable values (Fig. 4e, filled circles). SDW values were collected for the whole ontogeny and remain stable with a slightly increasing trend from three to nine chambers in the course of ontogeny (Fig. 4e, open circles). Measurements started close to the first septum and ended when reaching the final septum. Values for the septal spacing given in degrees are plotted against chamber number and not against the diameter in a linear, bivariate plot. First septa are characterized by high values close to 80° rapidly decreasing down to 30° at the fifth chamber. Afterward, the values remain more or less stable with slight, sinuous variation between 30° and 18°. Within the course of the last three septa, spacing slightly decreases down to 17°. Septa 14 (dm = 5.4 mm) and 21 (dm = 8.8 mm) show unexpectedly low values, i.e., lower

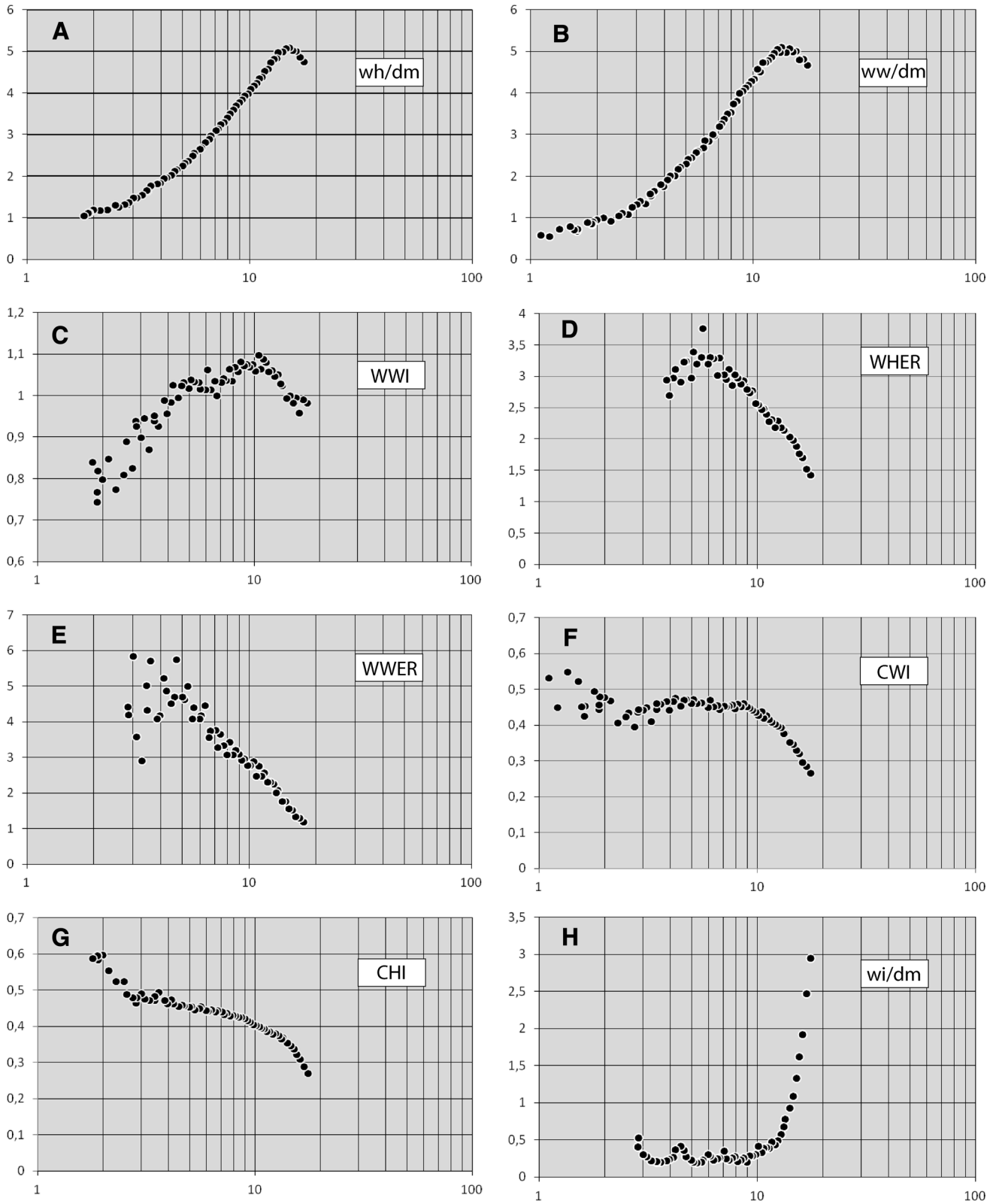

Fig. 3 Illustration of the ontogenetic development of the *Spirula spirula* shell. **a** Whorl height (wh). **b** Whorl width (ww). **c** Whorl width index (WWI). **d** Whorl height expansion rate (WHER). **e** Whorl width expansion rate (WWER). **f** Conch width index (CWI). **g** Conch height index (CHI). **h** Whorl interspace (wi). Diameter is plotted on the *x* axis

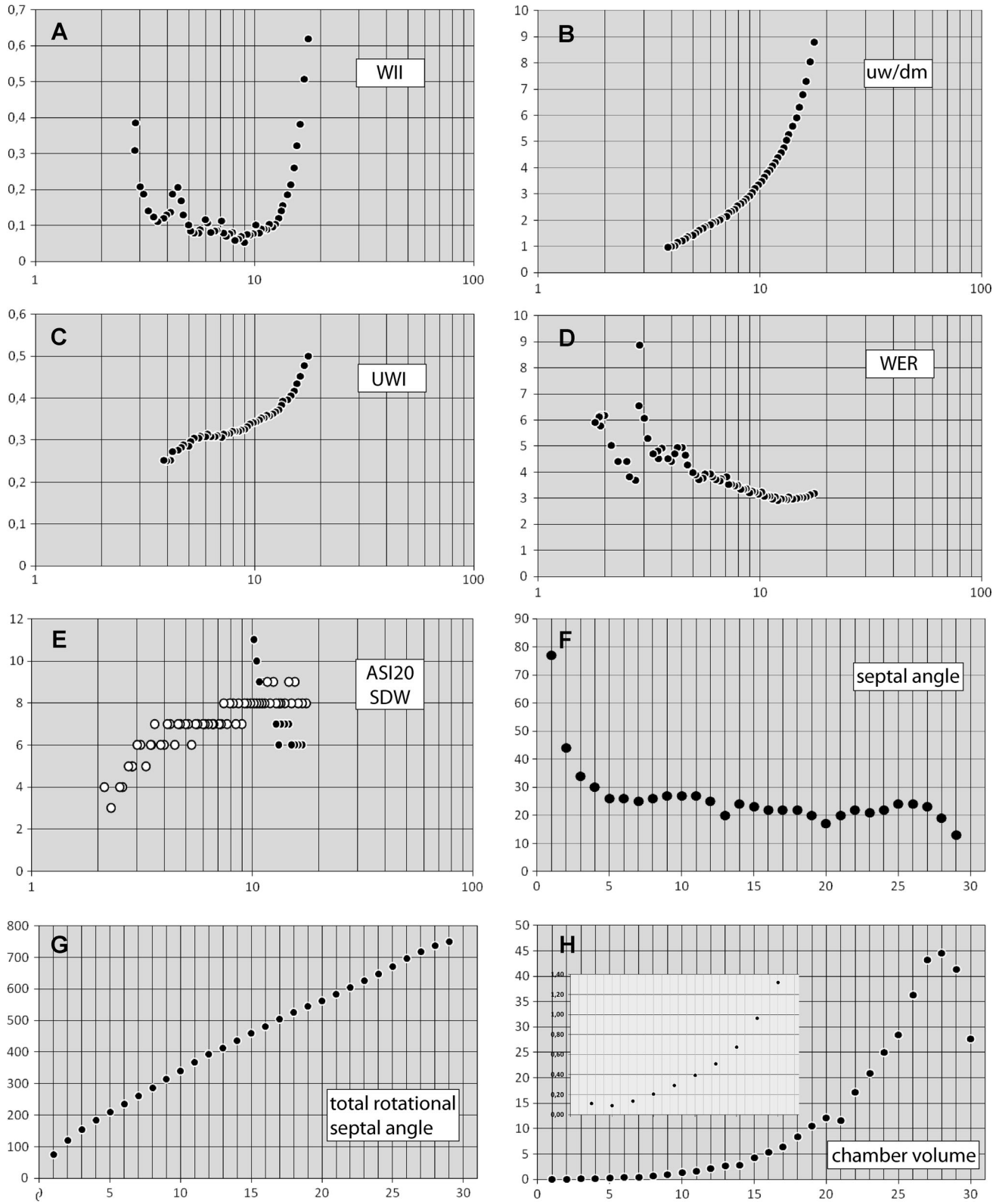

Fig. 4 Illustration of the ontogenetic development of the *Spirula spirula* shell. **a** Whorl interspace index (WII). **b** Umbilical width. **c** Umbilical width index (UWI). **d** Whorl expansion rate (WER). **e** Absolute septa index for a circle of 20-mm diameter (ASI_{20}, filled circles) and Septa per demiwhorl (SDW, open circles). **f** Septal distance in angles. **g** Total rotational angles. **h** Chamber volumes. **a–e** With the diameter plotted on the *x* axis, **f–h** Chamber number plotted on the *x* axis

than the values of the preceding and following septa (Fig. 4f). The total rotational graph starts with a very steep slope, which flattened at around the third septum and remains nearly constant throughout ontogeny (Fig. 4g).

Volume data

Volumes of the first ten chambers show only slight changes in volumes; therefore, an inset shows their volumes with a different scale. The initial chamber slightly exceeds the second chamber in volume. Chamber volumes begin to increase exponentially at about the 8th chamber. The last three chambers do not follow that trend. However, chamber 28 has the largest volume, while the volume of chamber 29 is smaller and that of the final chamber is reduced to a level comparable with that of chamber 25 (Figs. 4h, 5a). Ontogenetic development of the siphuncle volume follows a similar trend. Volume for the siphuncle in the initial chamber could not be collected. Volumes of later ontogenetic siphuncle portions show a larger scatter compared to corresponding chamber volumes (Fig. 5b). That scatter is related with the necessity to artificially close the siphuncular tube to separate a single siphuncle volume per chamber. It is assumed that different positions, due to the lack of a prominent morphological feature for a uniform placement, of the artificial closing to separate siphuncular volumes cause the scatter. The ratio of chamber volume and siphuncle surface area (CSI) increases during the early- and mid-stage of ontogeny to a maximum of nearly 160, i.e., the chamber volume exceeds the siphuncle volume by 160 times. At around the 22nd chamber, the ratio decreases reaching a value of 50 in the final chamber (Fig. 5c). Septal distances are plotted against chamber volumes showing a clear correlation trend between high values for septal angles and small chamber volumes during early ontogeny toward decreasing septal distances and increasing volumes in the course of ontogeny. During the final phase, septal distances and chamber volumes decrease (Fig. 4d).

Interpretation and discussion

The scatter in the presented graphs (WWI, WHER, WWER, CWI, and WER, Figs. 3c–f, 4d) of early ontogeny is potentially related to the morphology of the first chambers (strong curvature) or might be related with the defined center of the shell (Fig. 1c), which was determined as the dorsal attachment of the first septum by Neige and Warnke

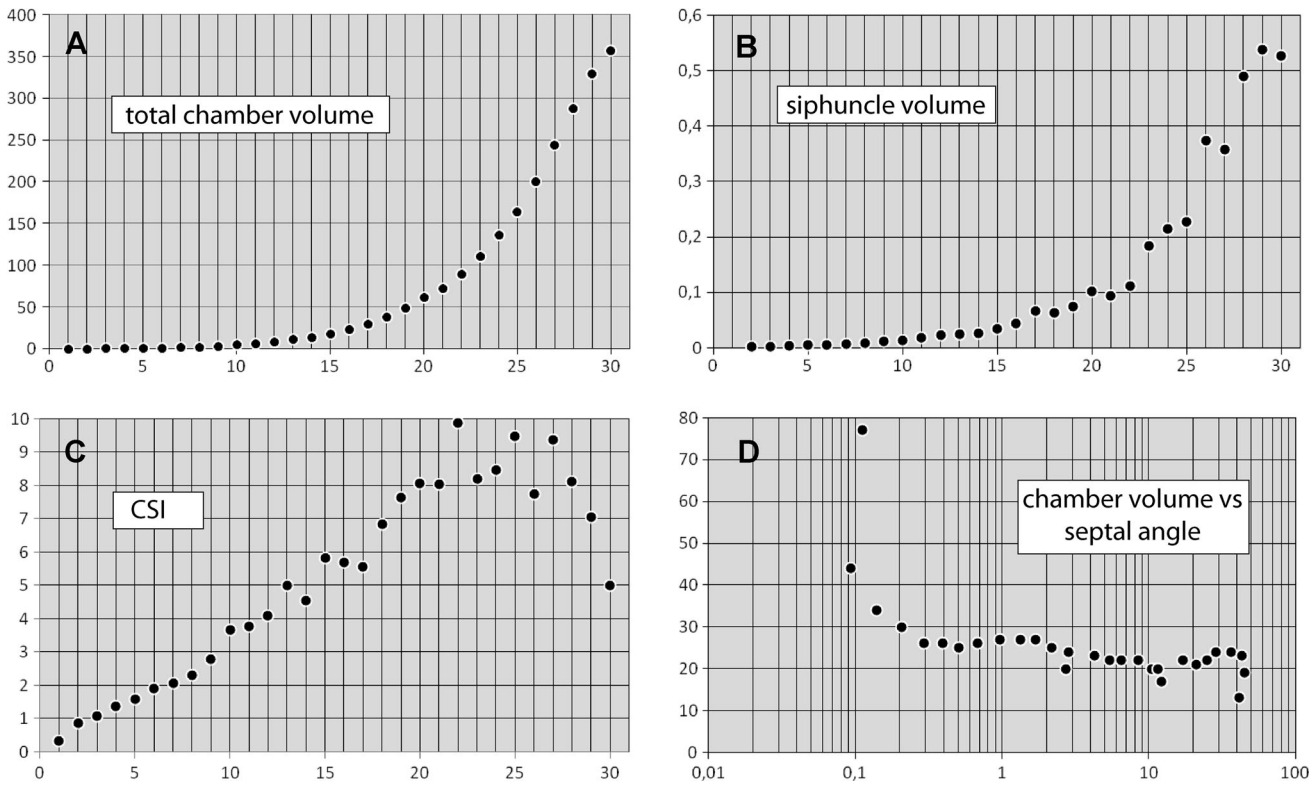

Fig. 5 Illustration of the ontogenetic development of the *Spirula spirula* shell. **a** Total chamber volume. **b** Siphuncle volume. **c**, Chamber volume against siphuncle surface area (CSI). **d** Septal angles plotted against chamber volumes show a clear three-phased trend. **a–d** With chamber numbers plotted on the *x* axis

(2010). By definition, this anatomical landmark does not describe the real center of the shell. In general, the potential error of 2D-measurements depends on the resolution, which is in this case 8.7 µm. Due to the high contrast, one may assume a deviation of measurements of 2–4 voxel at each end of the measured distances (4–8 in total), which results in a deviation 69.6 µm or 0.007 mm. Hence, the presented method provides 2D-data with sufficient precision. Volume data derived from computed tomographs are recorded as isotropic voxels, i.e., a 3D-pixel with identical dimensions in all three axes. Modern computed-tomographic-based volume reconstructions therefore lack one potential source of error: varying distances between subsequent slices leading to anisotropic voxels (variable dimensions at least in one direction, see Hoffmann et al. 2014).

Most of the 2D-measurements are used for the graphical description of cephalopod shell morphology and therefore largely contribute to the recognition of different species, ontogenetic changes, intraspecific variability, and macroevolutionary pattern. Here, we present a data mesh of 10° for all traditional conch parameters, which allows us to make a precise description of the shell geometry, a precise timing of ontogenetic changes, and the recognition of short-term changes. This is important because 2D-measurements provide biological signals, i.e., event of hatching, stressed environment, or terminal countdown morphology (Seilacher and Gunji 1993) indicating the adult stage.

For *Spirula*, the moment of hatching is still unknown (Hoffmann and Warnke 2014). Looking at the septal angle and the chamber volumes, one may speculate that hatching occurs after the second chamber was formed (Figs. 4f–h, 5d). This is based on a significant drop in the septal angle. Also, the chamber volumes show a slight decrease from the initial chamber to the second chamber followed by an increasing trend starting with the third chamber and ending with the 27th chamber (Fig. 4h). This fits very well with observations of young hatchlings with three chambers and a mantle length of about 2.7 mm (Bandel and Boletzky 1979). The adult stage is characterized by some special shell features summarized as terminal countdown morphology, a term coined by Seilacher and Gunji (1993). For *Spirula spirula*, we found the following terminal changes in shell morphology: (a) decreasing ww/wh ratio ending with a nearly circular cross section (Fig. 3c), (b) significant increase of the whorl interspace (Figs. 3h, 4a), (c) slight increase in the WER (Fig. 4d), and (d) septal crowding of the final two to three chambers (Fig. 4f) accompanied with a decrease in chamber volumes (Figs. 4h, 5d). Recognition of these features allows the identification of mature *Spirula* shells. Septal crowding (="Septendrängung" after Hölder 1956) was also reported for recent *Nautilus* by Ward (1987) and explained as a fine tuning of their buoyancy before growth stop of the shell and their soft body or as a compensation for the reduced density of the soft body resulting from the growth of the less-dense reproductive organs (Bucher et al. 1996). Septal crowding was also reported for extinct ammonoids and related to sexual maturity (Kraft et al. 2008 and references therein).

From our analysis, three conclusions can be drawn. First, unexpected changes in the chamber volume [chamber 14 (dm = 5.4 mm) and 21 (dm = 8.8 mm)] are not recorded by changes of the whorl height or whorl width (Fig. 3a–b) and do not correlate with any other abrupt changes in shell morphology but can be recognized by septal spacing (Figs. 2a–h, 3f, 4d).

Second, the herein presented *Spirula* shell shows a general trend of septal spacing starting with very high values (about 75°–30°) followed by a plateau phase with values varying between 30° and 20° and a final drop reaching values of 13° (Fig. 4f). The observed general trend was also reported by Neige and Warnke (2010). A similar tri-phasic trend of chamber volumes versus septal angles was reported for *Fidelites* by Naglik et al. (2015). The surface and the internal structure show no indication of pathology (injury, parasites, or disease). However, two chamber volumes (chambers 14 and 21) deviated from the expected trend in a probably premature stage. The graph presented by Neige and Warnke (2010, Fig. 3b) shows fluctuations of septal spacing in a probably premature stage. Little is known about these premature fluctuations in septal spacing, which are rarely investigated (see Kraft et al. 2008 and references therein). Because chambered cephalopods use their shells as a buoyancy device to compensate for their shell and soft tissue weight, it seems likely that changes of chamber volumes are related with growth of the aperture. This is based on the strong functional and constructional link between the formation of new septa and the apertural shell growth (Klug et al. 2008 and references therein). The herein reported unexpected reduction of two chamber volumes of a probably premature stage most likely indicates a growth disturbance due to external factors, i.e., a stressed environment (e.g., oxygen depletion, changes in sea water temperature, salinity, currents, or sea water chemical composition, reduced food availability or presence of predators) or internal factors (e.g., disease, parasites investing the soft body, see also Kraft et al. 2008 and Naglik et al. 2015). Based on shell examination, a reduction of septal spacing due to an injury or parasitism infesting, the shell is excluded. Those stress factors may prevent the *Spirula* animal from normal growth, i.e., increase in weight. As a consequence, a less positive buoyancy force is necessary resulting in smaller chamber volumes. Identification of distinct stress factors based on the chamber volume alone is not possible. However, other morphological characters, e.g., ww, wh,

WII, UWI, and WER, seem to be less sensitive to ecological changes and likely more related to the morphology of the soft tissue.

Third, we introduced the CSI as an indirect measurement of growth rate. If *Spirula* secreted a new chamber only after 50 % of the chamber liquid was removed, as reported for *Nautilus* by Ward (1987), that ratio is an independent measure for growth rate. In case the above-made assumptions are true, growth speed (chamber formation cycle) slows down until the 22nd chamber was formed and increases afterward until shell growth stops (Fig. 5c). Under the assumption that the morphology of siphuncular epithelia remained unchanged during cephalopod evolution (Kröger 2002, 2003), the CSI can be applied to extinct cephalopods. This allows for the comparison of relative growth rate in recent and extinct cephalopods.

Conclusions

Based on a beach finding of a *Spirula* shell, the potential application of non-invasive imaging techniques to the morphometric species description of the cephalopod shell was explored. It was demonstrated that volume data derived from micro-computed tomography can be used to obtain external and internal 2D-measurements (e.g., dm, uw, wh, and ww) and volume data with sufficient precision. Furthermore, tomographic data allow the development of a dense measurement grid (here 10°). It was found that relative changes in chamber volumes can be deduced from septal spacing. Unusual deviations from the expected ontogenetic trend of chamber volume development may indicate stressed environments. The ratio of chamber volume and siphuncle surface area acts as a proxy for growth speed. It is hoped that this method will be widely applied for the detection of intra- and interspecific variability in future cephalopod research.

Acknowledgments Svetlana Nikolaeva provided information about the deposition of Linné syntypes of *Spirula spirula*. Kerstin Warnke kindly donated a complete *Spirula* shell for this study. We thank the two reviewers for the comments improving an earlier version of this manuscript. RH and RL acknowledge financial support from the Deutsche Forschungsgemeinschaft (Grant Number HO 4674/2-1).

References

Bandel, K., & Boletzky, S. V. (1979). A comparative study of structure, development and morphological relationships of chambered cephalopod shells. *Veliger, 21*, 313–354.

Bucher, H., Landman, N.H., Guex, J., Klofak, S.M. (1996). Mode and rate of growth in ammonoids. In N.H. Landman, K. Tanabe, R.A. Davis (Eds.). Ammonoid Paleobiology. *Topics in Geobiology*, *13*, 407-461, New York, Plenum Press.

Dagys, A. S., & Weitschat, W. (1993). Extensive infraspecific variation in a Triassic ammonoid from Siberia. *Lethaia, 26*, 113–121.

De Baets, K., Klug, C., & Korn, D. (2009). Anetoceratinae (Ammonoidea, Early Devonian) from the Eifel and Harz Mountains (Germany), with a revision of their genera. *Neues Jahrbuch für Geologie und Paläontologie Abhandlungen, 252*, 361–376.

De Baets, K., Klug, C., Korn, D., & Landman, N. H. (2012). Early evolutionary trends in ammonoid embryonic development. *Evolution, 66*, 1788–1806.

De Baets, K., Klug, C., & Monnet, C. (2013). Intraspecific variability through ontogeny in early ammonoids. *Paleobiology, 39*, 75–94.

Hammer, O., & Bucher, H. (2005). Buckmańs first law of covariation—a case of proportionality. *Lethaia, 38*, 67–72.

Haring, E., Kruckenhauser, L., & Lukeneder, A. (2012). New DNA sequence data on the enigmatic *Spirula spirula* (Linnaeus, 1758) (Decabrachia, suborder Spirulina). *Ann Naturhist Mus Wien B, 113*, 37–48.

Hoffmann, R., Lemanis, R., Naglik, C., & Klug, C. (2015). Ammonoid buoyancy. In C. Klug, D. Korn, K. De Baets, I. Kruta, & R. H. Mapes (Eds.), *Ammonoid paleobiology* (Vol. I, p. 43). Germany: From Anatomy to Ecology Topics in Geobiology.

Hoffmann, R., Schultz, J. A., Schellhorn, R., Rybacki, E., Keupp, H., Gerden, S. R., et al. (2014). Non-invasive imaging methods applied to neo- and paleo- ontological cephalopod research. *Biogeosciences, 11*, 2721–2739.

Hoffmann, R., & Warnke, K. (2014). *Spirula*—das unbekannte Wesen aus der Tiefsee (*Spirula*—the unknown deep sea creature. *Denisia, 32*, 33–46.

Hohenegger, J., & Tatzreiter, F. (1992). Morphometric methods in determination of ammonite species, exemplified through *Balatonites* shells (Middle Triassic). *J Paleontol, 66*, 801–816.

Hölder, H. (1956). Über Anomalien an jurassischen Ammoniten. *Paläontologische Zeitschrift, 30*, 95–107.

Klug, C., Meyer, E., Richter, U., & Korn, D. (2008). Soft-tissue imprints in fossil and recent cephalopod septa and septum formation. *Lethaia, 41*, 477–492.

Korn, D. (2010). A key for the description of Palaeozoic ammonoids. *Fossil Record, 13*, 5–12.

Korn, D., & Klug, C. (2007). Conch form analysis, variability, morphological disparity, and mode of life of the frasnian (Late Devonian) ammonoid *Manticoceras* from coumiac (Montagne Noire, France). In N. H. Landman, R. A. Davis, & R. H. Mapes (Eds.), *Cephalopods Present and Past—New Insights and Fresh Perspectives* (pp. 57–85). Dordrecht: Springer.

Kraft, S., Korn, D., & Klug, C. (2008). Patterns of ontogenetic septal spacing in Carboniferus ammonoids. *Neues Jahrbuch für Geologie und Paläontologie Abhandlungen, 250*, 31–44.

Kröger, B. (2002). On the efficiency of the buoyancy apparatus in ammonoids: evidences from sublethal shell injuries. *Lethaia, 35*, 61–70.

Kröger, B. (2003). The size of the siphuncle in cephalopod evolution. *Senckenbergiana Lethaea, 83*, 39–52.

Kutygin, R. V. (1998). Forma rakovin permskikh ammonoidei severo-vostoka Rossii. *Paleontologicheskiy Zhurnal, 1998*(1), 20–31.

Landman, N. H., Kennedy, W. J., Cobban, W. A., & Larson, N. L. (2010). *Scaphites* of the "Nodosus Group" from the Upper Cretaceous (Campanian) of the western interior of North America. *Bulletin of the American Museum of Natural History, 342*, 1–242.

Lemanis, R., Zachow, S., Fusseis, F., & Hoffmann, R. (2015). A new approach using high-resolution computed tomography to test the buoyant properties of chambered cephalopod shells. *Paleobiology, 44*, 313–329. doi:10.1017/pab.2014.17.

Linnaeus, C., (1758). Systema naturae per regna tria naturae, secundum classes, ordines, genera, species cum characteribus, differentiis, synonymis, locis. *Editio decimal, reformata. Holmiae*.

Lukeneder, A., Harzhauser, M., Müllegger, S., & Piller, W. E. (2008). Stable isotopes ($\delta^{18}O$ and delta $\delta^{13}C$) in *Spirula spirula* shells from three major oceans indicate developmental changes paralleling depth distributions. *Marine Biology, 154*, 175–182.

Monnet, C., Bucher, H., Wasmer, M., & Guex, J. (2010). Revision of the genus *Acrochordiceras* Hyatt, 1877 (Ammonoidea, Middle Triassic): morphology, Biometry, Biostratigraphy and Intra-Specific Variability. *Palaeontology, 53*, 961–996.

Naglik, C., Monnet, C., Goetz, S., Kolb, C., De Baets, K., Tajika, A., & Klug, C. (2015). Growth trajectories of some major ammonoid subclades using grinding tomography data. *Lethaia, 48*, 29–46. doi:10.1111/let.12085.

Neige, P., & Warnke, K. (2010). Just how many species of *Spirula* are there? A morphometric approach. In K. Tanabe, Y. Shigeta, T. Sasaki, & H. Hirano (Eds.), *Cephalopods Present and Past* (pp. 57–85). Tokyo: Tokai University Press.

Ruzhencev, V. E. (1960). Printsipy sistematiki, sistema i filogeniya paleozoyskikh ammonoidey. *Trudy Paleontologicheskogo Instituta Akademia Nauk SSSR, 6*, 1–331.

Samadi, S., David, P., & Jarne, P. (2000). Variation of shell shape in the clonal snail *Melanoides tuberculata* and its consequences for the interpretation of fossil series. *Evolution, 54*, 492–502.

Scholz, H., & Glaubrecht, M. (2010). A new and open coiled *Valvata* (Gastropoda) from the Pliocene Koobi Fora formation of the Turkana Basin, Northern Kenya. *Journal of Palaeontology, 84*, 996–1002.

Seilacher, A., & Gunji, P. Y. (1993). Morphogenetic countdowns in heteromorph shells. *Neues Jahrbuch für Geologie und Paläontologie Abhandlungen, 190*, 237–265.

Tanabe, K. (1993). Variability and mode of evolution of the Middle Cretaceous Ammonite *Subprionocyclus* (Ammonitina: Collignoniceratidae) from Japan. *Geobios M.S., 15*, 347–357.

Teso, V., Signorelli, J. H., & Pastorino, G. (2011). Shell phenotypic variation in the south-western Atlantic gastropod *Olivancillaria carcellesi* (Mollusca: Olividae). *Journal of the Marine Biological Association of the United Kingdom., 91*, 1089–1094.

Ward, P. D. (1987). *The natural history of Nautilus*. London: Unwin Hyman.

Warnke, K. (2007). On the species status of *Spirula spirula* (Linné, 1758) (Cephalopoda): a new approach based on divergence of amino acid sequences between the canaries and new caledonia. In N. H. Landman, R. A. Davis, & R. H. Mapes (Eds.), *Cephalopods present and past—new insights and fresh perspectives* (pp. 144–155). Dordrecht: Springer.